Inorg. Chem. **2006**, *45*, 2972–2978

One Dense and Two Open Chiral Metal–Organic Frameworks: Crystal Structures and Physical Properties

Shuangquan Zang, Yang Su, Yizhi Li, Huizhen Zhu, and Qingjin Meng*

Coordination Chemistry Institute, State Key Laboratory of Coordination Chemistry, Nanjing University, Nanjing 210093, China

Received November 28, 2005

Three 3D robust homochiral helical coordination polymers, [Cu(2,2′,3,3′-H_2odpa)(bpy)] (**1**), {[Ni_4(2,2′,3,3′-odpa)$_2$(bpy)$_4$(H_2O)$_4$]·(H_2O)$_{16}$} (**2**), and {[Co_4(2,2′,3,3′-odpa)$_2$(bpy)$_4$(H_2O)$_4$]·(H_2O)$_{14}$} (**3**), have been hydrothermally synthesized from a flexible ligand of 2,2′,3,3′-odpda (2,2′,3,3′-oxydiphthalic dianhydride). Compound **1** crystallized in space group $P3_121$ and has a rare chiral dense qzd $7.^59$ topology that incorporates single helical substructures with the same accessibility, whereas compounds **2** and **3** crystallized in the space group *C*2 and possessed isostructural 3D chiral open frameworks based on the homochiral 2D sheets and 4,4′-bpy pillars. TGA and PXRD analyses show that the porous framework of **2** is stable after the removal of solvent water molecules. In contrast, **3** changed its structure to an amorphous one because of the simultaneous loss of solvent and coordination water molecules. **1** is nearly paramagnetic, whereas weak ferromagnetic interactions between M(II) (M = Ni, Co) ions have been found in **2** and **3**.

Introduction

The construction of novel coordination polymers is the current interest in the field of supramolecular chemistry and crystal engineering, stemming from their potential applications as functional materials[1−4] as well as their intriguing variety of architectures and molecular topologies.[5,6] In particular, solid materials with either helical or chiral structures are of intense interest in chemistry and material science.[6a,7,8] Although solid materials with unusual structures are expected to increase in number, the exploration for preparing framework solids with chiral structures still remains a challenge.[9−11]

As an important family of multidentate O-donor ligands, organic aromatic polycarboxylate ligands have been extensively employed in the preparation of metal−organic com-

* To whom correspondence should be addressed. E-mail: Mengqj@nju.edu.cn.

(1) (a) Leininger, S.; Olenyuk, B.; Stang, P. J. *Chem. Rev.* **2000**, *100*, 853. (b) Eddaoudi, M.; Moler, D. B.; Li, H. L.; Chen, B. L.; Reineke, T. M.; O'Keeffe, M.; Yaghi, O. M. *Acc. Chem. Res.* **2001**, *34*, 319. (c) Dybtsev, D. N.; Chun, H.; Yoon, S. H.; Kim, D.; Kim, K. *J. Am. Chem. Soc.* **2004**, *126*, 32. (d) Kitagawa, S.; Kitaura, R.; Noro, S. *Angew. Chem., Int. Ed.* **2004**, *43*, 2334.

(2) (a) Janiak, C. *J. Chem. Soc., Dalton Trans.* **2003**, 2781. (b) James, S. L. *Chem. Soc. Rev.* **2003**, *32*, 276. (C) Maspoch, D.; Ruiz-Molina, D.; Veciana, J. *J. Mater. Chem.* **2004**, *14*, 2713.

(3) (a) Evans, O.; Xiong, R. G.; Wang, Z.; Wong, G. K.; Lin, W. *Angew. Chem., Int. Ed.* **1999**, *38*, 536. (b) Evans, O. R.; Lin, W. *Acc. Chem. Res.* **2002**, *35*, 511.

(4) (a) Abrahams, B. F.; Jackson, P. A.; Roboson, R. *Angew. Chem., Int. Ed.* **1998**, *37*, 2656. (b) Abrahams, B. F.; Moylan, M.; Orchard, S. D.; Robson, R. *Angew. Chem., Int. Ed.* **2003**, *42*, 1848. (c) Qu, Z.-R.; Zhao, H.; Wang, Y.-P.; Wang, X.-S.; Ye, Q.; Li, Y.-H.; Xiong, R.-G.; Abrahams, B. F.; Liu, Z.-G.; Xue, Z.-L.; You, X.-Z. *Chem.—Eur. J.* **2004**, *10*, 53. (d) Xiong, R.-G.; Xue, X.; Zhao, H.; Abrahams, B. F.; You, X.-Z.; Xue, Z. *Angew. Chem., Int. Ed.* **2002**, *41*, 3800.

(5) (a) Wells, A. F. *Three-Dimensional Nets and Polyhedra*; Wiley-Interscience: New York, 1977. (b) Batten, S. R.; Robson, R. *Angew. Chem., Int. Ed.* **1998**, *37*, 1460. (c) Roboson, R. *J. Chem. Soc., Dalton. Trans.* **2000**, 3735. (d) Moulton, B.; Zaworoko, M. J. *Chem. Rev.* **2001**, *101*, 1629B. (e) Carlucci, L.; Ciani, G.; Proserpio, D. M. *Coord. Chem. Rev.* **2003**, *246*, 247. (f) Blatov, V. A.; Carlucci, L.; Cianib, G.; Proserpio, D. M. *CrystEngComm* **2004**, *6*, 377.

(6) (a) Bradshaw, D.; Claridge, J. B.; Cussen, E. J.; Prior, T. J.; Rosseinsky, M. J. *Acc. Chem. Res.* **2005**, *38*, 273. (b) Chou, J.-H.; Kosal, M. E.; Nakagaki, S.; Smithenry, D. W.; Wilson, S. R. *Acc. Chem. Res.* **2005**, *38*, 283. (c) Ockwig, N. W.; Delgado-Friedrichs, O.; O'Keefee, M.; Yaghi, O. M. *Acc. Chem. Res.* **2005**, *38*, 176. (d) Hill, R. J.; Long, D. L.; Champness, N. R.; Hubberstey, P.; Schroöder, M. *Acc. Chem. Res.* **2005**, *38*, *377*.

(7) (a) Piguet, C.; Bernardinelli, G.; Hopfgartner, G. *Chem. Rev.* **1997**, *97*, 2005. (b) Kesanli, B.; Lin, W.-B. *Coord. Chem. Rev.* **2003**, *246*, 305. (c) Bradsaw, D.; Prior, T. J.; Cussen, E. J.; Claridge, J. B.; Rosseinsky, M. J. *J. Am. Chem. Soc.* **2004**, *126*, 6106. (d) Lin, Z.; Jiang, F.; Chen, L.; Yuan, D.; Hong, M. *Inorg. Chem.* **2005**, *44*, 73.

(8) (a) Ellis, W. W.; Schmitz, M.; Arif, A. A.; Stang, P. J. *Inorg. Chem.* **2000**, *39*, 2547. (b) Prins, L. J.; Huskens, J.; Jong, F. D.; Timmerman, P. *Nature* **1999**, *398*, 498. (c) Chin, J.; Lee, S. S.; Lee, K. J.; Park, S.; Kim, D. H. *Nature* **1999**, *401*, 254. (d) Soghomonian, V.; Chen, Q.; Haushalter, R. C.; Zubieta, J.; O'Connor, C. J. *Science* **1993**, *259*, 1596.

(9) (a) Neeraj, S.; Natarajan, S.; Rao, C. N. R. *Chem. Commun.* **1999**, 165. (b) Monge, A.; Snejko, N.; Gutiérrez-Puebla, E.; Medina, M.; Cascales, C.; Ruiz-Valero, C.; Iglesias, M.; Gómez-Lor, B. *Chem. Commun.* **2005**, 1291.

10.1021/ic0520418 CCC: $33.50
Published on Web 02/25/2006

Chart 1. Structure of 2,2′3,3′-Odpda

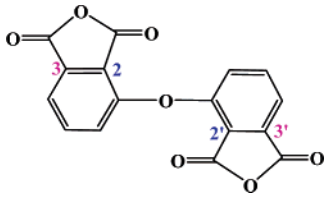

plexes that possess multidimensional networks and interesting properties.[12] On the other hand, it should be noted that the employment of flexible or V-shaped exomultidentate polycarboxylate ligands can improve the helicity of the polymeric chains.[11] Now, searching for this kind of versatile polycarboxylate ligand is very important and deserves attention in the investigation of new topologies and various functional materials.[11,13]

Among the reported network of metal carboxylates, 2,2′,3,3′-odpda[14] (Chart 1) remains largely unexplored. It was chosen as the multidentate ligand for the following reasons: (i) Hydrolysis of 2,2′,3,3′-odpda can produce multiple products of H_3odpa^-, H_2odpa^{2-}, $Hodpa^{3-}$, and $odpa^{4-}$, with the number of potential donor oxygen atoms varying from one to eight, which are all versatile ligands for the construction of novel high-dimensional metal−organic hybrid compounds. (ii) It can act not only as hydrogen-bond acceptor but also as hydrogen-bond donor, depending upon the number of deprotonated carboxyl groups. (iii) The flexibility around the etheric oxygen atom and the hindrances of the 2- and 2′-carboxylate groups provide the potential to form a helical coordination polymer. (iv) Upon the ligand being coordinated as a bridge, its freedom to rotate around the etheric oxygen atom is restrained and the ligand can be locked in a twisted chiral conformation. With the aim of understanding the coordination chemistry of this new versatile ligand and preparing new materials with interesting structural topologies and excellent physical properties, we have recently engaged in the research of coordination polymers based on 2,2′,3,3′-oxydiphthalic dianhydride (odpda) and 2,2′,3,3′-oxydiphthalic acid (H_4odpa). Employing this strategy, we have successfully obtained two novel d^{10} metal−organic coordination polymers from H_4odpa.[15] However, the change in metal centers may produce strikingly different structures. This idea prompted us to choose paramagnetic transition metal ions as the metal centers and bpy as an auxiliary ligand for constructing new metal−organic frameworks. Herein, we would like to present one dense and two open chiral MOFs and their properties.

Experimental Section

2,2′,3,3′-Odpada was synthesized according to the literature.[14] All other starting materials were of reagent quality and obtained from commercial sources without further purification.

[Cu(2,2′,3,3′-H_2odpa)(bpy)] (1). 1 was synthesized hydrothermally in a 23 mL Teflon-lined autoclave by heating a mixture of 0.1 mM 2,2′,3,3′-odpda, 0.1 mM bpy, 0.1 mM $Cu(NO_3)_2{\cdot}xH_2O$, and one drop of Et_3N (pH ≈ 7) at 120 °C for 2 days. Dark blue diamondlike single crystals were collected in 85% yield on the basis of copper. Anal. Calcd for $C_{26}H_{16}CuN_2O_9$: C, 55.37;H, 2.86; N, 4.97. Found: C, 55.35; H, 2.91; N, 4.91. IR (KBr, cm^{-1}): 3452 (vs), 3078 (vs), 2961 (vs), 1708 (s), 1614 (m), 1556 (s), 1444 (m), 1395 (s), 1251 (s), 1208 (s), 1192 (m), 1150 (w), 986 (w), 863 (w), 818 (m), 728 (m), 756 (m), 731 (w), 673 (m), 651 (w), 520 (m), 492 (w), 453 (w), 419 (w).

{[Ni_4(2,2′,3,3′-odpa)$_2$(bpy)$_4$(H_2O)$_4$]·(H_2O)$_{16}$} (2). 2 was synthesized hydrothermally in a 23 mL Teflon-lined autoclave by heating a mixture of 0.1 mmol of 2,2′,3,3′-odpada, 0.4 mM NaOH and 0.2 mmol of $Ni(NO_3)_2{\cdot}6H_2O$ at 120 °C for 2 days. Large, green, rectangular single crystals were collected in 75% yield on the basis of nickel. Anal. Calcd for $C_{72}H_{84}N_8Ni_4O_{38}$: C, 45.41; H, 4.44; N, 5.89. Found: C, 45.36; H, 4.49; N, 5.76. IR (KBr, cm^{-1}): 3420 (s, br), 2925 (vs), 2361 (s), 2341 (s), 1608 (s), 1561 (vs), 1541 (vs), 1526 (vs), 1471 (vs), 1413 (s), 1384 (s), 1282 (vs), 1236 (vs), 1073 (vs), 1047 (w), 996 (w), 818 (vs), 767 (vs), 638 (w), 501 (w), 419 (w), 504 (w), 374 (w), 320 (w).

{[Co_4(2,2′,3,3′-odpa)$_2$(bpy)$_4$(H_2O)$_4$]·(H_2O)$_{14}$} (3). 3 can also be obtained by following the same synthetic procedures as that for **2** except using $Co(NO_3)_2{\cdot}6H_2O$ instead of $Ni(NO_3)_2{\cdot}6H_2O$ as the starting material. Large, red, rectangular single crystals were collected in 67% yield on the basis of cobalt. Anal. Calcd for $C_{72}H_{80}N_8Co_4O_{36}$: C, 46.26; H, 4.31; N, 6.00. Found: C, 46.03; H, 4.82; N, 5.79. IR (KBr, cm^{-1}): 3421 (s, br), 2924 (vs), 2362 (s), 2341 (vs), 1606 (s), 1557 (s), 1460 (vs), 1393 (s), 1231 (vs), 1069 (vs), 815 (vs), 767 (w), 671 (w), 633 (w), 505 (w), 473 (w), 353 (w), 320 (w).

Physical Measurements. Elemental analyses were performed on a Perkin-Elmer 240C elemental analyzer. Powder X-ray diffraction patterns were recorded on a RigakuD/max-RA rotating anode X-ray diffractometer with graphite-monochromatic Cu Kα ($\lambda = 1.542$ Å) radiation at room temperature. The IR spectra were obtained as KBr disks on a VECTOR 22 spectrometer. Thermal analyses were performed on a TGA V5.1A Dupont 2100 instrument from room temperature to 700 °C with a heating rate of 10 °C/min in air. The circular dichroism (CD) spectra of **1**, **2**, and **3** were

(10) (a) Pérez-García, L.; Amabilino, D. B. *Chem. Soc. Rev.* **2002**, *31*, 342. (b) Wang, Y.-T.; Tong, M.-L.; Fan, H.-H.; Wang, H.-Z.; Chen, X.-M. *J. Chem. Soc., Dalton. Trans.* **2005**, 424. (c) Gao, E.-Q.; Bai, S.-Q.; Wang, Z.-M.; Yan, C.-H. *J. Am. Chem. Soc.* **2003**, *125*, 4984. (d) Wang, M.; Li, J. Y.; Yu, J. H.; Pan, Q. H.; Song, X. W.; Xu, R. R. *Inorg. Chem.* **2005**, *44*, 4604. (e) Moon, D.; Song, J.; Kim, B. J.; Jin, S. B.; Lah, M. S. *Inorg. Chem.* **2004**, *43*, 8230.

(11) (a) Tong, M.-L.; Cheng, X.-M.; Ye, B.-H.; Ng, S. W. *Inorg. Chem.* **1998**, *37*, 5278. (b) Carlucci, L.; Ciani, G.; Gramaccioli, A.; Proserpio, D. M.; Rizzato, S. *CrystEngComm* **2000**, 29. (c) Chen, X. M.; Liu, G. F. *Chem.—Eur. J.* **2002**, *8*, 4811. (d) Wang, X.-L.; Qin, C.; Wang, E.-B.; Xu, L.; Su, Z.-M.; Hu, C. W. *Angew. Chem., Int. Ed.* **2004**, *43*, 5036. (e) Wang, X.-L.; Qin, C.; Wang, E.-B.; Li, Y.-G.; Su, Z.-M. *Chem. Commun.* **2005**, 5450.

(12) (a) Li, H.; Eddaoudi, M.; O'Keeffe, M.; Yaghi, O. M. *Nature* **1999**, *402*, 276. (b) Chui, S. S.-Y.; Lo, S. M.-F.; Charmant, J. P. H.; Orpen, A. G.; Williams, I. D. *Science* **1999**, *283*, 1148. (c) Eddaoudi, M.; Kim, J.; Rosi, N.; Vodak, D.; Wachter, J.; O'Keefe, M.; Yaghi, O. M. *Science* **2002**, *295*, 469. (d) Eddaoudi, M.; Kim, J. *Nature* **2003**, *423*, 705. (e) Chael, H. K.; Siberio-Përez, D. Y.; Kim, J.; Go, Y. B.; Eddaoudi, M.; Matzger, A. J.; O'Keeffe, M.; Yaghi, O. M. *Nature* **2004**, *427*, 523. (f) Rao, C. N. R.; Natarajan, S.; Vaidhyanathan, R. *Angew. Chem., Int. Ed.* **2004**, *43*, 1466. (g) Rosi, N. L.; Kim, J.; Eddaoudi, M.; Chen, B.; O'Keeffe, M.; Yaghi, O. M. *J. Am. Chem. Soc.* **2005**, *127*, 1504.

(13) (a) Qi, Y.; Wang, Y.; Hu, C.; Cao, M.; Mao, L.; Wang, E. *Inorg. Chem.* **2003**, *42*, 8519. (b) Rueff, J.-M.; Pillet, S.; Claiser, N.; Bonaventure, G.; Souhassou, M.; Rabu, P. *Eur. J. Inorg. Chem.* **2002**, 895. (c) Wang, R. H.; Hong, M. C.; Luo, J. H.; Cao, R.; Weng, J. B. *Chem. Commun.* **2003**, 1018.

(14) Li, Q.-X.; Fang, X.-Z.; Wang, Z.; Gao, L.-X.; Ding, M.-X. *J. Polym. Sci., Part A: Polym. Chem.* **2003**, *41*, 3249.

(15) Zang, S.-Q.; Su, Y.; Li, Y.-Z.; Ni, Z.-P.; Meng, Q.-J. *Inorg. Chem.* **2006**, *45*, 174.

Table 1. Crystallographic Data and Refinement Parameters for **1**, **2**, and **3**

	1	2	3
formula	$C_{26}H_{16}CuN_2O_9$	$C_{72}H_{84}N_8Ni_4O_{38}$	$C_{72}H_{80}Co_4N_8O_{36}$
fw	563.95	1904.31	1869.16
cryst syst	trigonal	monoclinic	monoclinic
space group	$P3_121$	$C2$	$C2$
a (Å)	10.963(2)	24.444(1)	24.495(9)
b (Å)	10.963(2)	8.242(4)	8.320(2)
c (Å)	16.034(3)	11.259(5)	11.375(3)
α (deg)	90.0		
β (deg)	90.0	105.045(8)	105.222(1)
γ (deg)	120.0		
V (Å^3)	1668.8(5)	2190.5(2)	2237.0(1)
Z	3	1	1
ρ (g cm^{-1})	1.683	1.444	1.387
F(000)	861	988	964
GOF on F^2	0.995	1.065	1.078
R1, *wR2*[a] [$I > 2\sigma$(I)]	0.0650, 0.1523	0.0589, 0.1248	0.0577, 0.1710
R1, wR2[a] [all data]	0.0778, 0.1567	0.0768, 0.1288	0.0676, 0.1754
Flack	0.07(2)	0.02(2)	0.08(3)

[a] $R1 = \sum||F_o| - |F_c||/|F_o|$. $wR2 = [\sum w(\sum F_o^2 - F_c^2)^2/\sum w(F_o^2)^2]^{1/2}$.

recorded at room temperature with a JASCO J-810(S) spectropolarimeter (KBr pellets). Measurement of SHG response:[4d] The second-order nonlinear optical intensity was estimated by measuring a powder sample 80−150 μm in diameter in the form of a pellet relative to urea. A pulsed Q-switched Nd:YAG laser at a wavelength of 1064 nm was used to generate a SHG signal from powder samples. The backscattered SHG light was collected by a spherical concave mirror and passed through a filter that transmits only 532 nm radiation. Variable temperature magnetic susceptibility data were obtained on microcrystalline samples from 2 to 300 K in a magnetic field of 2 kOe, using a Quantum Design MPMSXL7 SQUID magnetometer. Diamagnetic corrections were made for both the sample holder and the compound estimated from Pascal's constants.[16]

X-ray Crystallographic Studies. Single crystals with dimensions 0.30 × 0.30 × 0.20 mm^3 for **1**, 0.30 × 0.20 × 0.20 mm^3 for **2**, and 0.30 × 0.26 × 0.22 mm^3 for **3** were used for structural determinations on a Bruker SMART APEX CCD diffractometer using graphite-monochromatized Mo Kα radiation (λ = 0.71073 Å) at room temperature using the ω-scan technique. Lorentz polarization and absorption corrections were applied. The structures were solved by direct methods and refined with the full-matrix least-squares technique using the SHELXS-97 and SHELXL-97 programs.[17] Anisotropic thermal parameters were assigned to all nonhydrogen atoms. Analytical expressions of neutral-atom scattering factors were employed, and anomalous dispersion corrections were incorporated. The crystallographic data and selected bond lengths for **1**, **2**, and **3** are listed in Tables 1 and 2.

Results and Discussion

Crystal Structures. [Cu(2,2′,3,3′-H$_2$odpa)(bpy)] (1). Single-crystal X-ray analysis revealed that **1** crystallizes in the space group $P3_121$ and has a chiral 3D structure constructed from Cu-odpa helical chains linked by bpy. As shown in Figure 1, each Cu^{II} center is in a square-planar geometry by coordinating to two nitrogen atoms (N1, N2) of *trans*-bpy and two oxygen atoms (O1, O1′) of two *trans*-2,2′3,3′-H$_2$odpa^{2-}. The 2,2′3,3′-H$_2$odpa^{2-} acts as a bis-monodentate ligand, and the dihedral angle between the two phenyl rings is 79.4°. The 2,2′-carboxylate groups are almost perpendicular to the plane of the correspondingly linked phenyl rings and 3,3′-carboxylate groups, with the dihedral angles between them being 98.1 and 95.0°, respectively. A visible twisting is also observed between two 2,2′-carboxylate groups in odpa, with the dihedral angle between them being 19.2°. The angle of C2O5C2′ is 119.7°. The combination of these twists and the nonlinear flexibility around the O5 atom results in the formation of a Cu-2,2′3,3′-H$_2$odpa helical chain. The helical chain's repeating unit, alongside a space-filling version, is shown in panels a and b of Figure 2.

Table 2. Selected Bond Lengths (Å) and Angles (deg) for **1**, **2**, and **3**

	Compound **1**[a]		
Cu(1)−O(1)	1.943(4)	Cu(1)−N(1)	1.947(7)
Cu(1)−N(2)	1.986(8)		
O(1)−Cu(1)−O(1)#1	178.6(3)	O(1)−Cu(1)−N(1)	90.68(13)
O(1)−Cu(1)−N(2)	89.32(13)		
	Compound **2**[b]		
Ni(1)−O(6)	2.034(4)	Ni(1)−O(4#2)	2.051(3)
Ni(1)−O(3)	2.055(4)	Ni(1)−O(1)	2.081(4)
Ni(1)−N(1)	2.058(4)	Ni(1)−N(2)	2.096(4)
O(6)−Ni(1)−O(4#2)	94.95(16)	O(6)−Ni(1)−O(3)	177.64(19)
O(4#2)−Ni(1)−O(3)	82.70(15)	O(6)−Ni(1)−N(1)	89.1(2)
O(4#2)−Ni(1)−N(1)	95.39(15)	O(3)−Ni(1)−N(1)	91.2(2)
O(6)−Ni(1)−O(1)	89.26(15)	O(4#2)−Ni(1)−O(1)	171.20(14)
O(3)−Ni(1)−O(1)	93.06(14)	N(1)−Ni(1)−O(1)	92.39(16)
O(6)−Ni(1)−N(2)	91.56(19)	O(4#2)−Ni(1)−N(2)	85.40(14)
O(3)−Ni(1)−N(2)	88.22(18)	N(1)−Ni(1)−N(2)	178.9(3)
O(1)−Ni(1)−N(2)	86.77(14)		
	Compound **3**[c]		
Co(1)−O(6)	2.030(5)	Co(1)−O(1)	2.086(4)
Co(1)−O(3)	2.084(5)	Co(1)−O(4#3)	2.072(4)
Co(1)−N(1)	2.155(5)	Co(1)−N(2)	2.173(5)
O(6)−Co(1)−O(4#3)	100.42(17)	O(6)−Co(1)−O(3)	173.21(18)
O(4#3)−Co(1)−O(3)	86.16(17)	O(6)−Co(1)−O(1)	84.01(16)
O(4#3)−Co(1)−O(1)	172.57(16)	O(3)−Co(1)−O(1)	89.62(17)
O(6)−Co(1)−N(1)	89.40(30)	O(4#3)−Co(1)−N(1)	93.66(17)
O(3)−Co(1)−N(1)	88.50(20)	O(1)−Co(1)−N(1)	92.33(18)
O(6)−Co(1)−N(2)	96.89(19)	O(4#3)−Co(1)−N(2)	85.37(17)
O(3)−Co(1)−N(2)	85.23(18)	O(1)−Co(1)−N(2)	88.19(17)
N(1)−Co(1)−N(2)	173.7(3)		

[a] Symmetry codes #1: $-x + 2, -x + y + 1, -z + 1/3$. [b] Symmetry codes #2: $-x + 1/2, y - 1/2, -z + 1$. [c] Symmetry codes #3: $-x + 1/2, y + 1/2, -z$.

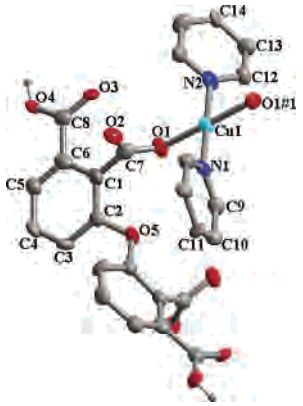

Figure 1. Molecular structure of **1**. Hydrogen atoms are omitted for clarity. #1: $1 - x, 1 - x + y, -2/3 - z$.

(16) Kahn, O. *Molecular Magnetism*; VCH Publishers: New York, 1993.
(17) (a) Sheldrick, G. M. *Acta Crystallogr., Sect. A* **1990**, *46*, 457. (b) Sheldrick, G. M. *SHELXL-97, Program for Crystal Structure Refinement*; University of Göttingen: Göttingen, Germany, 1997.

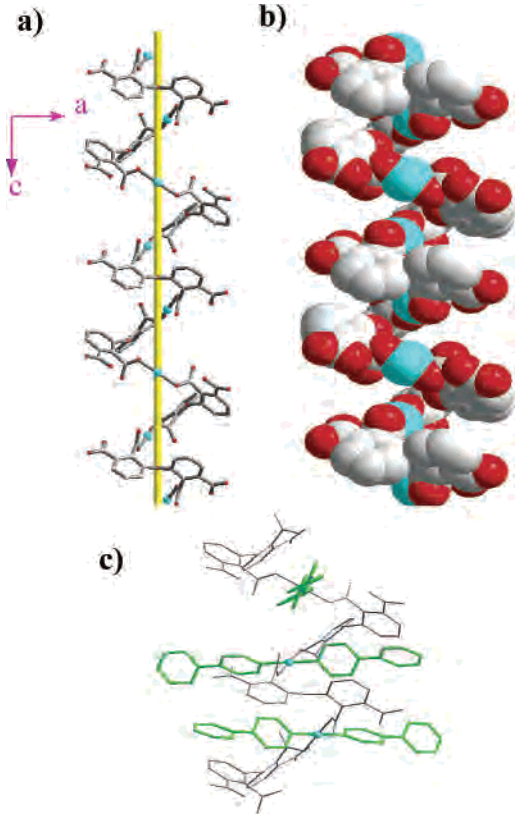

Figure 2. (a) Perspective view of a single 3_1 helical chain in **1**. (b) View of helical chain in space-filling modes. (c) Stereoview of a section of the helical chain including coordinational bpy molecules.

The winding axis corresponds to the *c*-axis, and the pitch to the length is 16.034(3) Å. The direction of rotation is a left-handed screw (*M*-helix). The single crystal consists of only homochiral helices. The shortest Cu−Cu distance between neighboring helices is 10.963 Å. Neighboring helices are united by both strong H-bonding (O4···O2 = 2.680Å, symmetry code: $-x + 1, -x + y + 1, -z + {}^1/_3$) and coordinational bpy. The full crystal packing in **1** is accomplished through Cu−bpy−Cu linkages between helices (Figure 2c). The bpy bridges are suitable for interleaving the neighboring chains and ensuring that acentric helices pack without introducing an inversion of center between them. In fact, bpy plays important roles both in forming the helical chain (see bellowing) and in homochiral helix assembly. With regard to homochiral helical chains assembled with the help of a second ligand, Poppelmeier and co-workers have first succeeded in obtaining the chiral materials on the basis of transition-metal oxylfluoride anions $[MO_2F_{6-x}]^{2-}$ and the second ligand pyrazine (M = V, Nb, Ta, $x = 1$; M = Mo, W, $x = 2$).[18] Their enlightening results revealed that a key to engineering noncentrosymmetric solids from acentric helices is the use of a short organic ligand to bridge the helices. In the case of **1**, the helix of the same handedness (left) shares identical spatial and translational orientation with other helices and therefore finds matching Cu−bpy−Cu bridges down the chain, as shown in Figure 3a. The bpy ligands orient in three directions (Figure 3a). Also, bpy adopts the

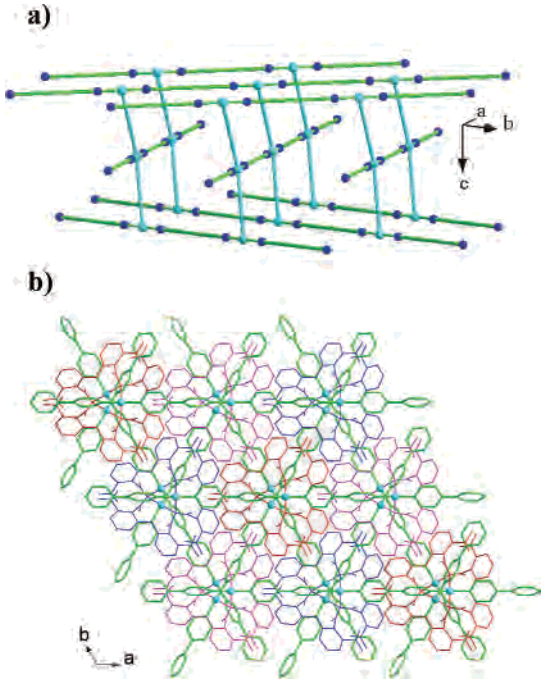

Figure 3. (a) Stereoview of the bpy arrangements (cyan sticks represent helices; green sticks represent three different orientations for bpy arrangements; blue and cyan dots represent nitrogen and copper atoms, respectively). (b) Crystal-packing illustration of **1** viewed along the *c*-axis (helices are presented as three different colors for clarity).

tortile conformation, with a dihedral angel of 41.4° between the two aromatic ring planes. A 3_1 screw axis can also be found down along the *c*-axis, according to bpy packing. Closed packing of bridged helices appears to be favored only when one-handed helices form in a single-crystal domain (Figure 3b). In fact, an efficient packing model with heterochiral helices cannot be obtained using the structural parameters of **1**.

Figure 3a also reveals a rare dense $7^5.9$ qzd network[5f,6c] displayed by this structure. The main feature of this net is that it is a dense $7^5.9$ net and incorporates helix substructures with the same accessibility. To the best of our knowledge, only a few dense $7^5.9$ qzd networks have been found up to now, including 3-fold interpenetrated[19] and single qzd networks.[18,20]

{[Ni$_4$(2,2′,3,3′-odpa)$_2$(bpy)$_4$(H$_2$O)$_4$]·(H$_2$O)$_{16}$} (2). Single-crystal X-ray analysis revealed that **2** crystallizes in the space group *C*2 and has a 3D chiral open framework based on homochiral sheets and 4,4′-bpy pillars. In **2**, two parts of odpa^{4-} ligands adopt a symmetric (ethetic oxygen atom O5 locked at the 2-fold axis) syn conformation. The dihedral angles between carboxylate groups and the correspondingly linked phenyl rings are 88.2° (2-COO$^-$ group) and 25.9° (3-COO$^-$ group), respectively. A dramatic twisting is observed between 2- and 3-carboxylate groups in odpa with a dihedral angle of 81.4°. As shown in Figure 4, each nickel atom is

(18) Maggard, P. A.; Stern, C. L.; Poeppelmeier, K. R. *J. Am. Chem. Soc.* **2001**, *123*, 7742.

(19) (a) Carlucci, L.; Ciani, G.; Macchi, P.; Proserpio, D. M. *Chem. Commun.* **1998**, 1837. (b) Withersby, M. A.; Blake, A. J.; Champness, N. R.; Hubberstey, P.; Li, W.-S.; Schroder, M. *Angew. Chem., Int. Ed.* **1997**, *36*, 2327.

(20) Zhang, J.; Kang, Y.; Zhang, R.-B.; Li, Z.-J.; Cheng, J.-K.; Yao, Y.-G. *CrystEngComm* **2005**, *7*, 177.

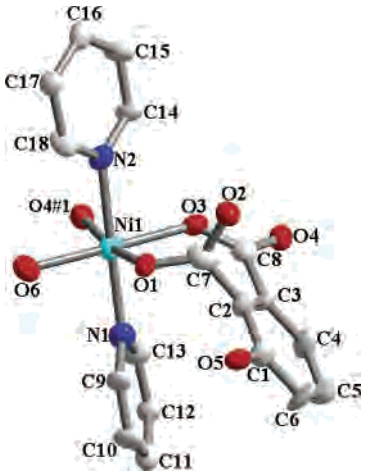

Figure 4. Unit structure of **2**. Hydrogen atoms and solvent water molecules are omitted for clarity. #1: $^1/_2 - x, -^1/_2 + y, 1 - z$.

six-coordinated by three oxygen atoms from 2,2′,3,3′-odpa^{4-} (O1, O3, and O4′), two nitrogen atoms from 4,4′-bpy (N1 and N2), and one oxygen atom from the coordinated water molecular (O6) in an octahedron geometry. **2** has a chiral 2D sheet structure in the *ab*-plane (Figure 5a), in which the Ni(II) ions are linked by *syn-anti* 3- or 3′-carboxylate groups from adjacent 2,2′,3,3′-odpa^{4-} ligands into infinite helical chains with a pitch of 8.242(4) Å along a 2_1 screw axis in the *b*-direction (Figure 5b). These chains are identified within the 2D sheet and crystallize spontaneously in a (*P*) right-handed fashion. Homochiral helix assembly in **2** is accomplished by the 2,2′,3,3′-odpa^{4-} ligand itself, in which the two phenyl rings are united together by the etheric oxygen atom (O5). First, the screw of carboxylate groups resulted in the formation of the helical chain, and then the homochiral information can be effectively transferred through the etheric oxygen atom (O5). Swallowlike chiral open channels with approximate dimensions 8.2 × 8.2 Å^2 are generated along the *c*-axis direction (Figure 5a).

Another outstanding feature in **2** is that these 2D chiral layers can be supported by the second rigid ligands to form another kind of channel with approximate dimensions 9.5 × 11.3 Å^2, estimated using the Ni−Ni separations on the edges as shown in Figure 5c. Solvent water molecules occupy the holes through hydrogen bonds (see the Supporting Information, Table S1). The void volume for **2**, as calculated by PLATON[21] from the crystal structures, is 31%. As far as our understanding of chiral porous MOFs goes, **2** is a rare example that is constructed from mixed-ligand methods.[22]

A better insight into the nature of this interesting framework can be achieved by the application of topological approach, i.e., reducing multidimensional structures to simple node-and-connection nets. Taking the Ni atoms as nodes and connections between metal centers as rods, the single framework topology representation for **2** parallel to the *ab*-plane is illustrated in Figure 6a. The net of this single

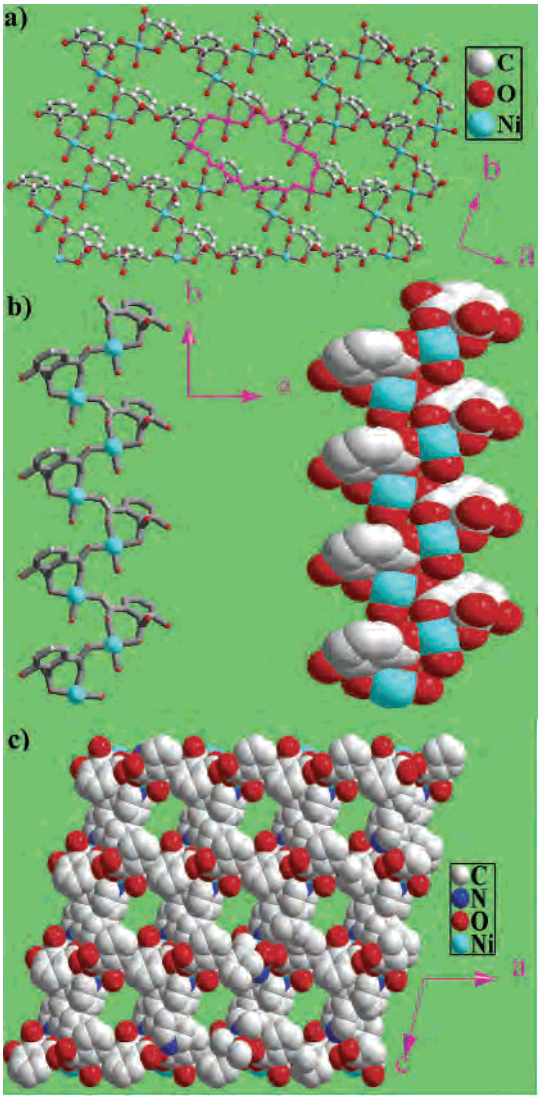

Figure 5. (a) Two-dimensional chiral sheet. One swallowlike chiral channel is marked as purple. (b) One *P* helical chain along the *b*-axis. (c) Space-filling model to show the channels along the *b*-axis direction.

framework can be described as a 6^3 topology. These 6^3 nets are linked together through bpy molecules to give a five-connected 3D network (Figure 6b).

{[Co$_4$(2,2′,3,3′-odpa)$_2$(bpy)$_4$(H$_2$O)$_4$]·(H$_2$O)$_{14}$} (3). Compound **3** is isostructural with **2** except that the number of noncoordinating water molecules/formula unit of **3** is less than that of **2**.

According to the above structural description of our example compounds, two kinds of hydrolysis products of odpa are found. In **1**, H$_2$odpda^{2-} acts as flexibility ligand coordinating to Cu^{2+} ions to obtain a helical chain, in which the hindrance of 2 and 2′-carboxylate groups play important roles in the formation of the helix. These helical chains can then be assembled to give a 3D homochiral helical coordination polymer through both hydrogen bonds and the direction of the second ligand bpy. In **2** and **3**, odpa^{4-} ligands coordinate to metal centers in a mutichelating fashion to form a 2D chiral sheet, in which the helical chains are derived from the screws of the carbolylate groups. In a 2D level, homochiral transfer can be accomplished through the ligand

(21) Spek, A. L. *PLATON, Amultipurose Crystallographic Tool*; Utrecht University: Ultrecht, The Netherlands, 2001.
(22) (a) Ma, B. Q.; Mulfort, K. L.; Hupp, J. T.*Inorg. Chem.* **2005**, *44*, 4912. (b) Wang, X.-L.; Qin, C.; Wang, E.-B.; Li, Y.-G.; Hu, C.-W.; Xu, L. *Chem. Commun.* **2004**, 378.

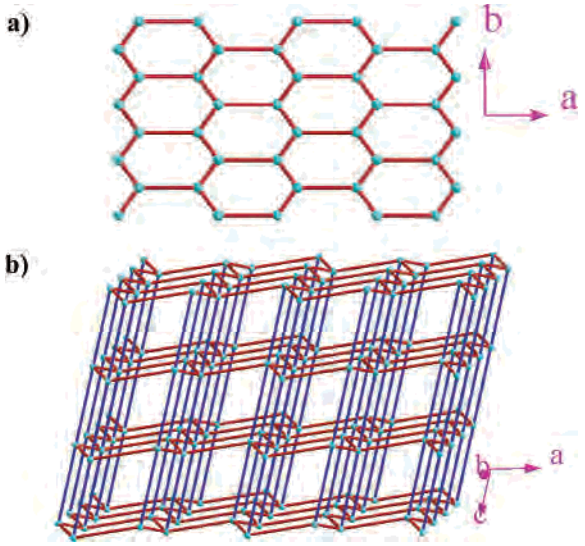

Figure 6. (a) Topological view of the 6^3 net in **2**. (b) The interconnected 6^3 nets of **2** (intralayer red, interlayer blue).

itself. Bpy molecules act as pillars to support the 2D chiral layers and to give a 3D chiral porous metal−organic framework.

Although the screws of the carbolylate groups are also the major reason for the formation of helices in our Zn- and Cd-odpa complexes,[15] the situation is very different. In **2** and **3**, two parts of the $odpa^{4-}$ ligands adopt a symmetric syn conformation to coordinate to Ni^{2+} (or Co^{2+}) ions and give a brick wall topology, whereas they adopt an asymmetric anti conformation to coordinate to Zn^{2+} (or Cd^{2+}) ions and give a puckered herringbone motif in which each part of $odpa^{4-}$ discriminates only one of the two crystallographically nonequivalent Zn or Cd atoms. In addition, in our Zn- and Cd-odpa complexes, bpy molecules strengthened the chiral herringbone motifs in the same layer.

Thermal Analyses and PXRD Patterns. A thermogravimetric analysis of complex **1** displays no weight loss between 25 and 250 °C. The decomposition of complex **1** starts above 250 °C (see the Supporting Information, Figure S1). Thermogravimetric analysis (TGA) for crystal samples of **2** shows that a weight loss of 14.81% in the range 25−150 °C corresponds to a loss of the uncoordinated water molecules (calculated at 15.14% for $4{\cdot}H_2O$ per one nickel atom), whereas the loss of coordinated water occurs above 200 °C, as shown in the Supporting Information, Figure S2. In contrast, a weight loss of 18.13% indicates that both the solvent and coordinated water molecules (calculated at 17.35% for $5{\cdot}H_2O$ per one cobalt atom) are lost in the range 5−120 °C for compound **3** (see the Supporting Information, Figure S3).

To further test the stability of the porous frameworks of **2** and **3**, we examined the powder samples of **2** and **3** by X-ray diffraction analysis. Guest water molecules were removed by heating **2** and **3** at 150 °C for 2 h. Powder X-ray diffraction patterns of as-synthesized **2** and dehydrated samples are nearly identical (Figure 7), which indicates that the porous framework can stably exist even with the loss of guest water molecules. However, the framework of **3** is

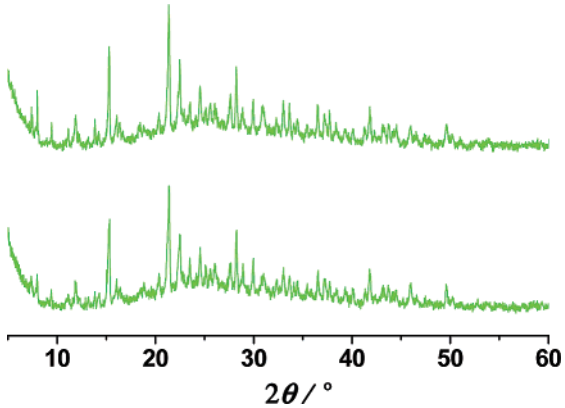

Figure 7. PXRD patterns for **2**. Top: taken at room temperature; down: after heating to 150 °C for 2 h.

destroyed when subjected to the loss of water molecules (see the Suppporting Information, Figure S4), and the sample changes its color from red to magenta. This phenomenon can be understood because the coordination water molecules are lost at the same time as the solvent water is lost.

Though the losses of water molecules are usually correlative with hydrogen bonds, they cannot give any reasonable information about the difference thermal stabilities between compounds **2** and **3**.

SHG Activity. Though each crystal may give a pronounced Cotton effect in its CD spectra (usually opposite at random) for materials derived from spontaneous resolution from achiral compounds, bulk materials for **1**, **2**, and **3** show no visible Cotton effect in their CD spectra. However, a chiral network is itself noncentrosymmetric, so our bulk materials are acentric materials that have a potential application as NLO-active materials. We have performed quasi-Kurtz second-harmonic-generation measurements on powder samples to confirm their acentricity as well as to evaluate their potential application in second-order NLO material.[23] Preliminary experimental results show that the bulk materials display modest powder SHG efficiency approximately 0.7, 0.4, and 0.1 times that of urea for **1**, **2**, and **3**, respectively.

Magnetic Properties. The global feature of the $\chi_m T$ vs T curve of **1** is a very weak antiferromagnetic interaction (see the Supporting Information, Figure S5). The value of $\chi_m T$ at 300 K is 0.416 emu K mol^{-1}, which is as expected for one uncoupled copper(II) ion. The $\chi_m T$ values are constant in the entire temperature range, decreasing to a value of 0.408 emu K mol^{-1} at very low temperatures. The $\chi_m{}^{-1}$ vs T plot is almost linear in the entire temperature range as shown in the inset of Figure S5 (see the Supporting Information). The shape of these curves is a typical one for the Curie law. The data were therefore analyzed by the Curie−Weiss law, which led to the parameters $C = 0.415$ emu K mol^{-1} and $\theta = -0.072$ K, corresponding to the parameter $g = 2.104$. The small θ value indicates the very weak antiferromagnetic interactions between Cu^{II} ions, and the superexchange parameter can be related to the nature of the bridging among the neighbor copper(II) atoms.

(23) Kurtz, S. K. *J. Appl. Phys.* **1968**, *39*, 3798.

Figure S6 of the Supporting Information shows the magnetic behavior of **2** in the form of a $\chi_m T$ vs T plot. At 300 K, $\chi_m T$ is 1.219 emu K mol $^{-1}$ per nickel(II). Upon **2** being cooled to 24.0 K, the $\chi_m T$ values increase continuously to a maximum of 1.273 emu K mol^{-1}, indicating the presence of ferromagnetic coupling in **2**. Upon further cooling of **2** below 24.0 K, the $\chi_m T$ values decrease, to 0.839 emu K mol^{-1} at 1.8 K, which could be due to the antiferromagnetic interactions through 4,4′-bpy [2a] and/or the zero-field splitting of the ground state. The χ_m^{-1} vs T is almost linear through the whole temperature range (see the Supporting Information, inset of Figure S6). The data were therefore analyzed by the Curie−Weiss law, which led to parameters $C = 1.2303$ emu K mol^{-1} and $\theta = 0.9338$. The small θ value indicates weak ferromagnetic interactions in **2**, which have also been witnessed in other *syn-anti* carboxylate bridged nickel(II) complexes.[24]

For **3**, the $\chi_m T$ value is 3.11 emu K mol^{-1} at 300 K, decreases to a minimum of 2.16 cm^3 K mol^{-1} at 10 K, and then increases abruptly to 2.36 emu K mol^{-1} at 2 K (see the Supporting Information, Figure S7). Fitting the data above 30 K using the Curie−Weiss law gives a Curie constant $C = 3.299$ emu K mol^{-1}, significantly larger than the spin-only value of 1.875 emu K mol^{-1} for cobalt(II) ($S = 3/2$), and a negative Weiss constant $\theta = -15.48$ K. Commonly, this kind of behavior of $\chi_m T$ and the negative θ value may indicate the occurrence of a dominant antiferromagnetic coupling between the spin carriers. However, the spin−orbit coupling of the $^4T_{1g}$ state of the cobalt(II) ion in an octahedral ligand field can normally lead to a negative θ value and a decrease in $\chi_m T$ at high temperatures. Thus, the increase in $\chi_m T$ below 10 K may indicate the possibility for ferromagnetic coupling between metal centers (see the Supporting Information).[25]

The design of chiral magnetic materials combining magnetism and optical activity is one of the major challenges in the pursuit of polyfunctional materials.[26,27] It is expected that chiral magnets, which usually have relatively large magnetic moments, may open the possibility for observing stronger MChD effects.[10c,28] A few chiral molecular magnets, all based on coordination polymers, have been prepared, although their MChD effects and spin structures in the chiral and magnetically ordered phases remain to be explored.[10c,28−29]

Conclusion

In summary, a versatile achiral ligand of 2,2′,3,3′-odpda has been introduced that constructs transition-metal-containing chiral coordination polymers. When it reacts with Cu^{II} with the help of bpy in the presence of weak alkali metals, a chiral dense $7^5.9$ qzd network (**1**) is obtained. During the investigation of the reaction between 2,2′,3,3′-odpda and other paramagnetic transition-metal ions (Ni (II) and Co (II)), two isostructural 3D chiral porous frameworks (**2** and **3**) were also obtained. In addition, **2** has a permanent porous metal−organic framework subject to the loss of guest solvent water molecules. Following studies will focus on the construction of new chiral metal−organic coordination polymers from this ligand and its isomers.

Acknowledgment. We are grateful for financial support from the State Basic Research Project and the National Natural Science Foundation of China. The authors also thank Prof R.-G. Xiong for his kind help.

Supporting Information Available: Additional crystallographic graphs, TG curves, PXRD patterns, χ_mT−T curves, χ_m^{-1}−T curves, and X-ray crystallographic files in CIF format for the structure determination of compounds **1**, **2**, and **3**. This material is available free of charge via the Internet at http://pubs.acs.org.

IC0520418

(24) (a) Wu, C. D.; Lu, C. Z.; Yang, W. B.; Zhuang, H. H.; Huang, J. S. *Inorg. Chem.* **2002**, *41*, 3302. (b) Whitfield, T.; Zheng, L.; Wang, M. X.; Jacobson, A. J. *Solid State Sci.* **2001**, *3*, 829.
(25) Sun, H.-L.; Wang, Z.-M.; Gao, S. *Inorg. Chem.* **2005**, *44*, 2169.
(26) Coronado, E.; Palacio, F.; Veciana, J. *Angew. Chem., Int. Ed.* **2003**, *42* , 2570.
(27) (a) Rikken, G. L. J. A.; Raupach, E. *Nature* **1997**, *390*, 493. (b) Rikken, G. L. J. A.; Raupach, E. *Nature* **2000**, *405*, 932.
(28) Gao, E.-Q.; Yue, Y.-F.; Bai, S.-Q.; He, Zheng.; Yan, C.-H. *J. Am. Chem. Soc.* **2004**, *126*, 1419.
(29) (a) Inoue, K.; Kikuchi, K.; Ohba, M.; Okawa, H. *Angew. Chem., Int. Ed.* **2003**, *42*, 4810. (b) Minguet, M.; Luneau, D.; Lhotel, E.; Villar, V.; Paulsen, C.; Amabilino, D. B.; Veciana, J. *Angew. Chem., Int. Ed.* **2002**, *41*, 586. (c) Caneschi, A.; Gatteschi, D.; Ray, P.; Sessoli, R. *Inorg. Chem.* **1991**, *30*, 3936. (d) Han, S.; Manson, J. L.; Kim, J.; Miller, J. *Inorg. Chem.* **2000**, *39*, 4182.